

Generalized parton distributions from form factors*

M. Diehl^a

^aDeutsches Elektronen-Synchrotron DESY, 22603 Hamburg, Germany

The electromagnetic nucleon form factors provide constraints on generalized quark distributions. Key results of the study presented here are a strong dependence of the average impact parameter of quarks on their longitudinal momentum fraction, a striking difference in the t dependence of u and d quark contributions to elastic form factors, and an estimate of the orbital angular momentum carried by valence quarks in the nucleon.

1. INTRODUCTION

Much of what we know about hadron structure comes from measurements of parton densities, which quantify the distribution of longitudinal momentum and helicity of partons in a fast-moving hadron. Generalized parton distributions (GPDs) complement this essentially one-dimensional picture with information in the plane perpendicular to the direction of movement. These distributions parameterize matrix elements of non-local quark or gluon operators. We focus here on the unpolarized quark sector, where the distribution $H^q(x, \xi, t)$ is diagonal in proton helicity and $E^q(x, \xi, t)$ describes proton helicity flip. The variables x and ξ parameterize longitudinal quark momentum fractions relative to the average proton momentum $\frac{1}{2}(p + p')$ as shown in Fig. 1, whereas the invariant $t = (p - p')^2$ depends on both longitudinal and transverse components of the momentum transferred to the proton. In the forward limit $p = p'$ one recovers the usual quark and antiquark densities as $q(x) = H^q(x, 0, 0)$ and $\bar{q}(x) = -H^q(-x, 0, 0)$ with $x > 0$. For the precise definitions of GPDs and further information we refer to the recent reviews [1].

According to factorization theorems, GPDs appear in the scattering amplitudes of suitable hard exclusive processes such as deeply virtual Compton scattering, $\gamma^* p \rightarrow \gamma p$, and exclusive meson production, e.g. $\gamma^* p \rightarrow \rho p$. In these processes,

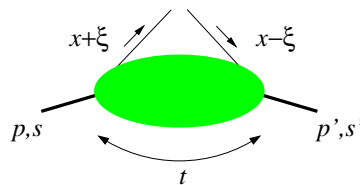


Figure 1. Relevant variables in a GPD.

the longitudinal momentum transfer ξ is fixed by the kinematics, whereas x is a loop variable. To disentangle the x and ξ dependence of GPDs from measured process amplitudes remains an outstanding task, but generically the dominating values of x in the loop integrals will be of order ξ .

2. IMPACT PARAMETER DENSITIES

To represent GPDs in transverse position space, we form wave packets

$$|p^+, \mathbf{b}\rangle = \int \frac{d^2\mathbf{p}}{(2\pi)^2} e^{-i\mathbf{b}\mathbf{p}} |p^+, \mathbf{p}\rangle \quad (1)$$

from momentum eigenstates $|p^+, \mathbf{p}\rangle$, where we write $v^\pm = (v^0 \pm v^3)/\sqrt{2}$ for the light-cone components and $\mathbf{v} = (v^1, v^2)$ for the transverse part of a four-vector v . The state $|p^+, \mathbf{b}\rangle$ is localized at \mathbf{b} in the transverse plane (often called impact parameter plane). Formally it is an eigenstate of a suitably defined transverse position operator [2]. It is thus possible to localize a relativistic state exactly in *two* dimensions, whereas localization in all *three* dimensions involves ambiguities at the level of the Compton wavelength. For

*To appear in: Procs. of the Workshop on Light-Cone QCD and Nonperturbative Hadron Physics 2005 (LC 2005), Cairns, Australia, 2005

a parton interpretation it is natural to consider states $|p^+, \mathbf{b}\rangle$ with large p^+ , which describe a fast-moving proton. Further analysis reveals that \mathbf{b} is the “center of momentum” of the partons in the proton, given as $\mathbf{b} = \sum_i p_i^+ \mathbf{b}_i / \sum_i p_i^+$ in terms of their plus-momenta and transverse positions. The center of momentum is related by Noether’s theorem to transverse boosts, in analogy to the relation between the center of mass and Galilean transformations in nonrelativistic mechanics.

Taking matrix elements between impact parameter states (1) of the quark or gluon operators defining general parton distributions in momentum space, one obtains Fourier transforms of these distributions. For vanishing skewness parameter ξ one finds that

$$q(x, \mathbf{b}) = \int \frac{d^2 \Delta}{(2\pi)^2} e^{-i\mathbf{b}\Delta} H^q(x, 0, -\Delta^2) \quad (2)$$

is the density of quarks with longitudinal momentum fraction x and transverse distance \mathbf{b} from the center of momentum of the proton [3]. For nonzero ξ one no longer has a probability interpretation because the two quark momentum fractions in Fig. 1 are not the same, but \mathbf{b} still describes the distribution of the struck quark in the transverse plane [4]. According to the discussion at the end of the introduction, the combined ξ and t dependence of hard exclusive scattering processes thus yields information about the impact parameter distribution of partons with longitudinal momentum fraction of order ξ . Note that the connection between GPDs and spatial distributions in the transverse plane discussed here differs from the well-known representation of form factors in terms of spatial distributions in *three* dimensions, which has been extended to GPDs in [5].

Just as the ordinary parton densities, the distributions $q(x, \mathbf{b})$ depend on the scale μ at which the partons are resolved. The scale evolution is local in \mathbf{b} and described by the usual DGLAP equations. For the valence quark distributions $q_v(x, \mathbf{b}) = q(x, \mathbf{b}) - \bar{q}(x, \mathbf{b})$ we have

$$\mu^2 \frac{d}{d\mu^2} q_v(x, \mathbf{b}) = \int_x^1 \frac{dz}{z} \left[P\left(\frac{x}{z}\right) \right]_+ q_v(z, \mathbf{b}), \quad (3)$$

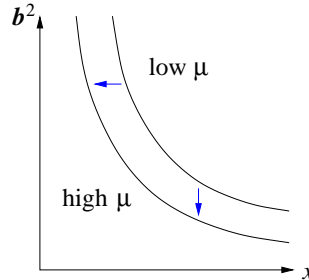


Figure 2. Typical pattern of scale evolution in x and \mathbf{b}^2 .

where $P(z)$ denotes the quark splitting function. As a consequence the \mathbf{b} dependence of the distributions at given x changes with μ . In particular, the average squared impact parameter $\langle \mathbf{b}^2 \rangle_x$ for valence quark distributions evolves as [6]

$$\begin{aligned} \mu^2 \frac{d}{d\mu^2} \langle \mathbf{b}^2 \rangle_x & \\ &= - \frac{1}{q_v(x)} \int_x^1 \frac{dz}{z} P\left(\frac{x}{z}\right) q_v(z) \left[\langle \mathbf{b}^2 \rangle_x - \langle \mathbf{b}^2 \rangle_z \right], \end{aligned} \quad (4)$$

where we defined

$$\begin{aligned} \langle \mathbf{b}^2 \rangle_x &= \frac{\int d^2 \mathbf{b} \mathbf{b}^2 q_v(x, \mathbf{b})}{\int d^2 \mathbf{b} q_v(x, \mathbf{b})} \\ &= 4 \frac{\partial}{\partial t} \log H_v^q(x, t) \Big|_{t=0} \end{aligned} \quad (5)$$

with $H_v^q(x, t) = H^q(x, 0, t) + H^q(-x, 0, t)$ being the momentum space counterpart of $q_v(x, \mathbf{b})$. The evolution equations for singlet distributions mix quarks and gluons as usual. We will argue below that $\langle \mathbf{b}^2 \rangle_x$ is a decreasing function of x . Since $P(z) > 0$, the average impact parameter at given x then decreases with μ according to (4). This is readily understood: at fixed \mathbf{b} evolution to higher scale μ decreases the longitudinal momentum of quarks because they radiate gluons. As sketched in Fig. 2, this implies a smaller typical \mathbf{b} at given x as μ increases.

At large x , the struck quark takes most of the proton momentum, so that its impact parameter tends to coincide with the center of momentum of the entire proton. In the limit $x \rightarrow 1$ one thus expects a narrow distribution in \mathbf{b} , or equivalently a flat t dependence of GPDs in momentum space.

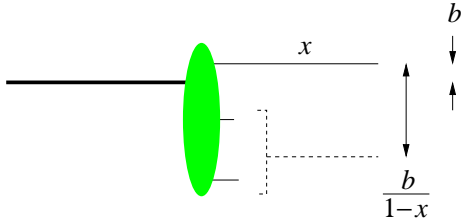


Figure 3. Three-quark configuration with one fast quark in a proton. The thick line denotes the center of momentum of the proton and the dashed line the center of momentum of the two spectator quarks.

An estimate for the overall transverse size of the proton in that limit is provided by the transverse distance $\mathbf{b}/(1-x)$ between the struck quark and the center of momentum of the *spectator* partons, as shown in Fig. 3. It is plausible to assume that this distance remains finite due to confinement [7], so that the average squared impact parameter of partons vanishes like $\langle \mathbf{b}^2 \rangle_x \sim (1-x)^2$ for $x \rightarrow 1$.

3. THE DIRAC FORM FACTORS

Information on the interplay between x and t in the valence distributions $H_v^q(x, t)$ can be obtained from the Dirac form factors of proton and neutron via the sum rules

$$F_1^p(t) = \int_0^1 dx \left[\frac{2}{3} H_v^u(x, t) - \frac{1}{3} H_v^d(x, t) \right], \quad (6)$$

$$F_1^n(t) = \int_0^1 dx \left[\frac{2}{3} H_v^d(x, t) - \frac{1}{3} H_v^u(x, t) \right], \quad (7)$$

where we have neglected the contribution from strange quarks. Flavor labels in H_v^q refer to quarks in the proton. Notice that the dependence of GPDs on the resolution scale μ cancels in these integrals, because the electromagnetic form factors belong to a conserved current. In this way, form factors measured at low t can constrain the distributions of partons resolved at much higher resolution scales μ^2 .

The information from elastic form factors is very complementary to what can be learned from hard exclusive scattering processes. Experimental coverage in t and the precision of measurements and their quantitative interpretation is

typically greater for form factors than for more complex exclusive processes. Electromagnetic form factors are sensitive to the difference of quark and antiquark distributions and thus insensitive to sea quarks and gluons, which can be accessed in processes like deeply virtual Compton scattering or vector meson production. Finally, parton momentum fractions only appear under an integral in elastic form factors, whereas a combined measurement of the ξ and t dependence in exclusive processes gives a more direct correlation of longitudinal and transverse variables as discussed in Sect. 2.

3.1. An ansatz for the distribution H_v^q

In the following we present results of the analysis of electromagnetic form factors performed in Ref. [6], to which we refer for details. A study along similar lines can be found in [8]. Our ansatz for H_v^q is of the form

$$H_v^q(x, t) = q_v(x) \exp[t f_q(x)], \quad (8)$$

where for $q_v(x)$ we have taken the CTEQ6M parameterization [9]. The results of our analysis are stable within the CTEQ error estimates on the parton densities. All distributions in the following refer to the scale $\mu = 2$ GeV. The interplay between x and t dependence in H_v^q is controlled by the profile function $f_q(x)$, which according to (5) is readily identified as $\frac{1}{4} \langle \mathbf{b}^2 \rangle_x$.

For small x , Regge phenomenology of soft hadronic interactions suggests an ansatz [10]

$$H_v^q(x, t) \sim x^{-(\alpha+\alpha't)} = x^{-\alpha} e^{t\alpha' \log(1/x)} \quad (9)$$

for the x dependence, with $\alpha \approx 0.4$ to 0.5 and $\alpha' \approx 0.9$ GeV $^{-2}$ corresponding to the leading meson exchange trajectories. This is known to work rather well for the usual valence quark densities, i.e. in the forward limit $t = 0$. We note that in the singlet sector the situation is more complicated: the powers α parameterizing sea quark and gluon densities at scales of a few GeV are significantly larger than the respective values for meson and pomeron exchange in soft hadronic reactions. Furthermore, the value of α' measured in exclusive J/Ψ production, which involves the generalized gluon distribution, is smaller than the corresponding value for pomeron exchange in soft

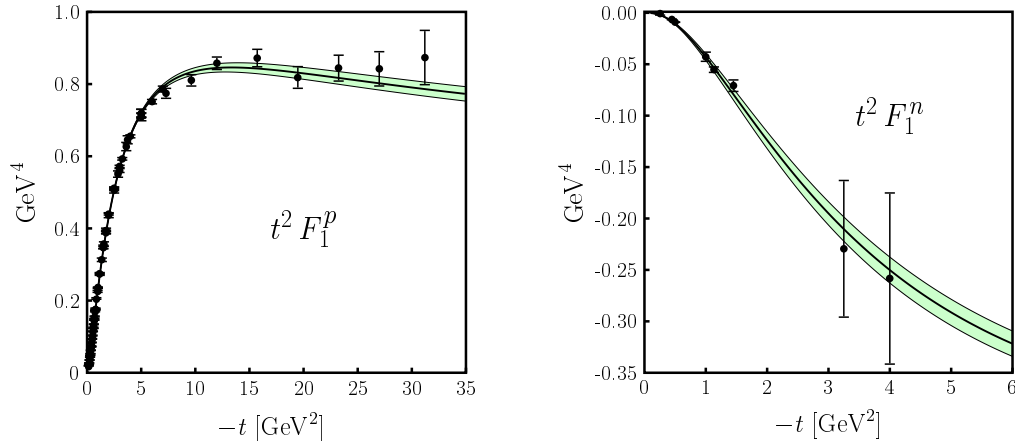


Figure 4. Results of fitting the ansatz given by (8) and (10) to the proton and neutron Dirac form factors using the sum rules (6) and (7). Shaded bands reflect the $1\text{-}\sigma$ uncertainties on the fitted parameters. The data for F_1^p are described within 5% except for the point at the highest $|t|$.

scattering processes [11]. It remains an outstanding task to constrain the shrinkage parameter α' in generalized sea quark distributions and to understand its interplay with α' for gluons through evolution in μ .

For the limit $x \rightarrow 1$ we impose $f_q(x) \sim (1-x)^2$, corresponding to a finite transverse size of the proton as discussed in Sect. 2. We investigated several forms of f_q that interpolate between the limiting behavior for $x \rightarrow 0$ and $x \rightarrow 1$ just discussed, and found good results with

$$f_q(x) = \alpha'(1-x)^3 \log(1/x) + B_q(1-x)^3 + A_q x(1-x)^2. \quad (10)$$

The high power of $(1-x)$ multiplying the term with $\log(1/x)$ ensures that the parameter α' controls the behavior of the distribution at small but not at moderate or large x – we expect that the physics in these x regions is very different and not naturally described by the same parameters.

3.2. Results and lessons of the fit

With the ansatz just described we obtain a good fit to the data for the Dirac form factors, as seen in Fig. 4. To reduce the number of free parameters we set $\alpha' = 0.9 \text{ GeV}^{-2}$; leaving it free we find $\alpha' = 0.97 \pm 0.04 \text{ GeV}^{-2}$ well in the region suggested by Regge phenomenology. We also im-

posed $B_u = B_d$; relaxing this constraint improves the fit only slightly. The main result of our fit is a strong x dependence of the average impact parameter of valence quarks over the entire x range. This is illustrated for u quarks in Fig. 5, where we plot the average distance d_u between struck quark and spectators.

We have also fitted the form factors to the alternative ansatz

$$f_q(x) = \alpha'(1-x)^2 \log(1/x) + B_q(1-x)^2 + A_q x(1-x) \quad (11)$$

for the profile function. This leads to a similarly good description of the data as with the form (10). The reason can be seen in Fig. 5. Up to $x \sim 0.8$ the fitted results for $d_u(x)$ are barely distinguishable; only for larger x does the fit with (11) produce a rise of $d_u(x)$ to values that appear unphysically large. In the t range where there is data, the form factor F_1^p is however barely sensitive to $x > 0.8$. This is shown in Fig. 6, where we also plot the average value

$$\langle x \rangle_t = \frac{\sum_q e_q \int_0^1 dx x H_v^q(x, t)}{\sum_q e_q \int_0^1 dx H_v^q(x, t)} \quad (12)$$

of x in the integral (6). The more scarce data on F_1^n do not constrain the region $x > 0.8$ either.

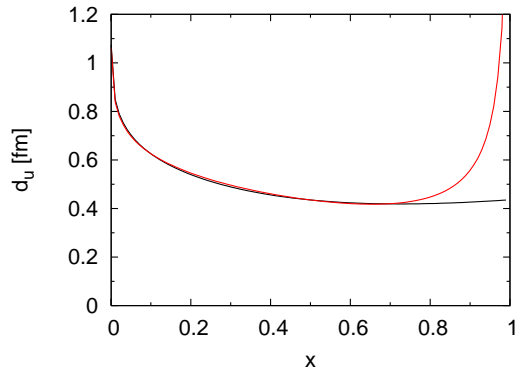


Figure 5. Average distance between struck quark and spectators in the valence distribution for u quarks, given by $d_u = (1-x)^{-1} [(b^2)_x]^{1/2}$ according to Fig. 3. The lower curve is for our fit (10) and the upper one for the alternative fit (11).

We see from this exercise that with observables sensitive to $x \lesssim 0.8$ one cannot unambiguously determine a power-law behavior in $(1-x)$ for the limit $x \rightarrow 1$.

The average impact parameter for d quarks is less well constrained by our fit since F_1^p , for which data is abundant, is dominated by u quarks. We found however that a good description of the F_1^n data requires a larger impact parameter of d quarks compared with u quarks at moderate to large x . It will be interesting to see whether future data on F_1^n confirm this trend. This would be an analog to the very different distribution in x of u and d quarks, which may for instance hint at a quark-diquark structure of nucleon configurations at large x [12].

3.3. Large t : Feynman and Drell-Yan

If one assumes that elastic form factors are dominated by configurations where partons not struck by the photon have virtualities of the order of a strong interaction scale Λ^2 , then at large t the momentum fraction of the struck quark must become large – this is the mechanism originally proposed by Feynman [12]. The integrals (6) and (7) are then dominated by the region where $1-x \sim \Lambda/\sqrt{-t}$. The large- t asymptotics of our ansatz (8) and (10) indeed follows this behavior,

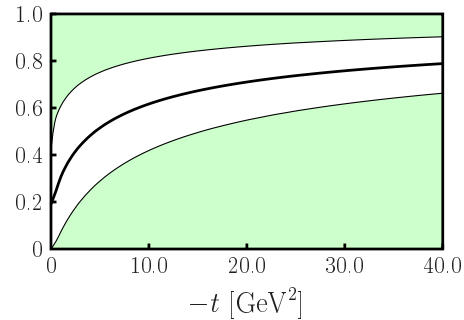


Figure 6. Region of x (white region) which accounts for 90% of $F_1^p(t)$ in the integral (6) for our fit of $H_v^q(x, t)$. The upper and lower shaded x -regions each account for 5% of $F_1^p(t)$. The thick line shows the average $\langle x \rangle_t$ as defined in (12).

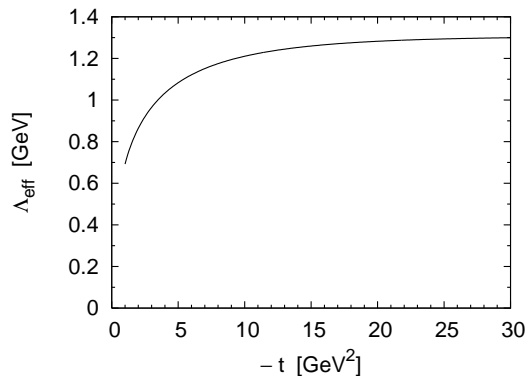


Figure 7. The scale parameter Λ_{eff} for the Feynman mechanism, as explained in the text.

as is readily seen from the saddle point approximation of the relevant integrals. To quantify this we have evaluated $\Lambda_{\text{eff}}(t) = \sqrt{-t} \langle 1-x \rangle_t$ with $\langle 1-x \rangle_t = 1 - \langle x \rangle_t$ from (12). The result is displayed in Fig. 7 and shows that the expected asymptotic behavior slowly sets in for $|t|$ around 10 GeV^2 .

To explore the dependence of our conclusions on the assumed form of $H_v^q(x, t)$, we have performed fits with the exponential t dependence in (8) replaced by a power law

$$H_v^q(x, t) = q_v(x) \left(1 - \frac{t f_q(x)}{p} \right)^{-p} \quad (13)$$

with $f_q(x)$ of the form (10). We obtain a good description of the form factors in a wide range of p , from $p \approx 2.5$ up to the limit $p \rightarrow \infty$, where we recover the exponential (8). Asymptotically, our modified ansatz still satisfies $\langle 1-x \rangle_t \sim \Lambda/\sqrt{-t}$. For small p this behavior is however not reached at values of t where there is data, and the form factor sum rules are not dominated by large x . (This underlines the need to check asymptotic considerations against numerical estimates when describing baryon form factors.) The available data for F_1^p does hence *not prove* that the Feynman mechanism is at work in the high- t region, but it is *consistent* with this assumption, given the success of our fits with large p .

Dominance of the Feynman mechanism implies the Drell-Yan relation

$$F_1^q(t) \sim |t|^{-(1+\beta_q)/2} \quad \text{for } q_v(x) \sim (1-x)^{\beta_q} \quad (14)$$

between the form factors $F_1^q(t) = \int dx H_v^q(x, t)$ at large t and parton distributions at large x . We can understand β_q as an *effective* power describing the behavior of $q_v(x)$ at large x (rather than in the experimentally unexplored limit $x \rightarrow 1$). With the CTEQ6M distributions at $\mu = 2$ GeV we find $u_v(x) \sim (1-x)^{3.4}$ and $d_v(x) \sim (1-x)^{5.0}$ for $0.5 \leq x \leq 0.9$. The Drell-Yan relation then implies a drastically different t dependence of the contributions from u and d quarks to the nucleon form factors. $F_1^u = 2F_1^p + F_1^n$ should approximately scale like $|t|^{-2}$ at large t , whereas $F_1^d = F_1^p + 2F_1^n$ should fall off like $|t|^{-3}$. This difference in the large- t behavior is already felt at lower values of t , as can be seen in the two upper panels of Fig. 8, where we plot the x moments

$$h_i^q(t) = \int_0^1 dx x^{i-1} H_v^q(x, t) \quad (15)$$

with $i = 1, 2, 3$ for the GPDs obtained in our fit. The lowest moments h_1^u and h_1^d can be extracted from experimental data on the electromagnetic proton and neutron form factors, and the higher moments are accessible to calculation in lattice QCD [13,14,15]. Both types of studies are challenging for $|t|$ above 3 GeV^2 , where our fit predicts the most striking differences between u and d quarks, but will hopefully be feasible in the future.

4. THE PAULI FORM FACTORS

The proton helicity flip distributions E^q admit a density interpretation at $\xi = 0$, similar to the distributions H^q discussed so far. To see this one changes basis from proton helicity states $|\uparrow\rangle, |\downarrow\rangle$ to states $|X\pm\rangle = (|\uparrow\rangle \pm |\downarrow\rangle)/\sqrt{2}$ polarized along the positive or negative x axis. In impact parameter space one then obtains the density

$$q_X(x, \mathbf{b}) = q(x, \mathbf{b}) - \frac{b^y}{m} \frac{\partial}{\partial \mathbf{b}^2} e^q(x, \mathbf{b}) \quad (16)$$

of unpolarized quarks in a proton polarized in the positive x direction, where $q(x, \mathbf{b})$ and

$$e^q(x, \mathbf{b}) = \int \frac{d^2 \Delta}{(2\pi)^2} e^{-i\mathbf{b}\Delta} E^q(x, 0, -\Delta^2) \quad (17)$$

depend on \mathbf{b} only through \mathbf{b}^2 due to rotation invariance. The impact parameter distribution of quarks in a transversely polarized proton is thus shifted in the direction perpendicular to the polarization. The interpretation of (16) as a density implies positivity bounds for $e^q(x, \mathbf{b})$, which in momentum space can be written as [16]

$$\begin{aligned} & \left[E^q(x, 0, t=0) \right]^2 \quad (18) \\ & \leq m^2 \left[q(x) + \Delta q(x) \right] \left[q(x) - \Delta q(x) \right] \\ & \quad \times 4 \frac{\partial}{\partial t} \log \left[H^q(x, 0, t) \pm \tilde{H}^q(x, 0, t) \right]_{t=0}. \end{aligned}$$

Depending on the sign, the term in the third line is the average squared impact parameter of quarks with positive or negative helicity, which according to our previous discussion tends to zero for large x . In addition, the densities $d + \Delta d$ and $u - \Delta u$ of right-handed d and left-handed u quarks are phenomenologically known to decrease strongly with x , so that the right-hand side of (18) restricts $|E^q(x, 0, 0)|$ quite severely for larger values of x . The distribution E^q involves one unit of orbital angular momentum since in the associated matrix elements the proton helicity is flipped but the quark helicity conserved, see Fig. 9. The bound (18) thus limits the amount of orbital angular momentum that can be carried by quarks with large x .

Sum rules analogous to (6) and (7) relate the Pauli form factors of proton and neutron with

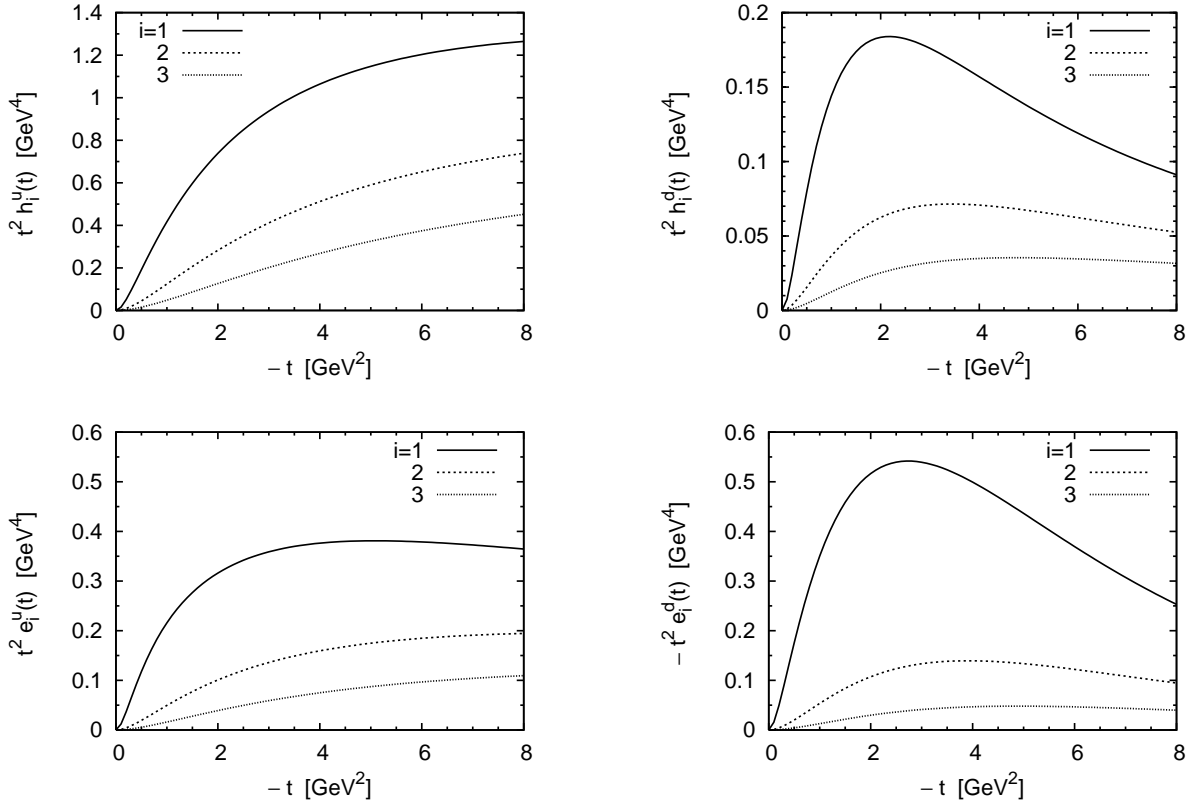


Figure 8. Scaled x moments (15) and (23) of generalized u and d valence distributions at $\mu = 2$ GeV, obtained from our fits described in Sects. 3.1 and 4.

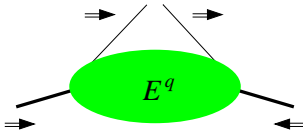


Figure 9. E^q describes transitions where the proton helicity is flipped but the quark helicity conserved. The helicity mismatch is compensated by one unit of orbital angular momentum, according to angular momentum conservation.

the valence combinations $E_v^q(x, t) = E^q(x, 0, t) + E^q(-x, 0, t)$ of proton helicity flip distributions. These distributions cannot be measured at $t = 0$ so that in contrast to $H_v^q(x, t)$ their forward limit is unknown. We have made an ansatz

$$E_v^q(x, t) = e_v^q(x) \exp[tg_q(x)] \quad (19)$$

with $g_q(x)$ of the same functional form as $f_q(x)$ in (10). For the forward limit of E_v^q we assumed a form

$$e_v^q(x) = \mathcal{N}_q x^{-\alpha} (1-x)^{\beta_q}, \quad (20)$$

which is known to work quite well for the ordinary valence quark distributions $q_v(x)$. The normalization factors \mathcal{N}_q are fixed by the requirement $\int dx e_v^q(x) = \kappa_q$ with $\kappa_u \approx 1.67$ and $\kappa_d \approx -2.03$ obtained from the magnetic moments of proton and neutron. The overall normalization of E_v^q is

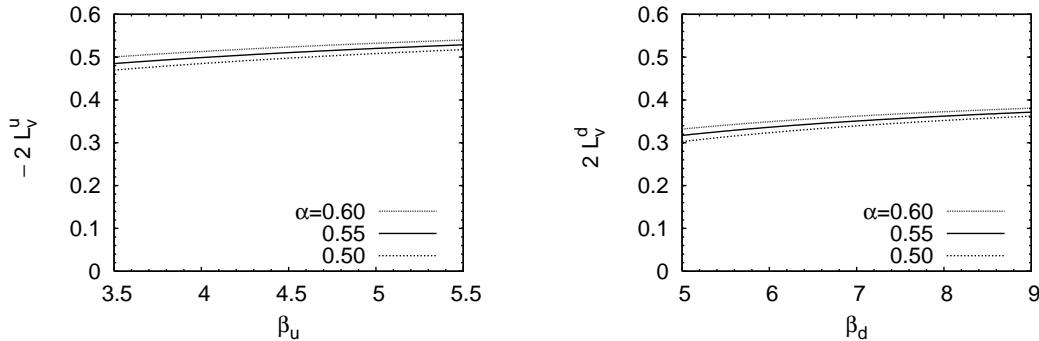


Figure 10. The orbital angular momentum carried by valence quarks at scale $\mu = 2$ GeV, obtained in the range of parameters for which we obtain a good fit to the proton and neutron Pauli form factors. The corresponding values for the total angular momentum $J_v^q = L_v^q + \frac{1}{2} \int dx \Delta q_v(x)$ are $J_u = L_u + \frac{1}{2} 0.93$ and $J_v^d = L_v^d - \frac{1}{2} 0.34$, so that J_v^d comes out close to zero in our estimate.

hence quite large, which according to our discussion implies significant spin-orbit effects of u and d quarks in the proton.

Using the ansatz just described we obtain a good fit to the data for the Pauli form factors of proton and neutron, with $\alpha = 0.55$ and $\alpha' = 0.9$ GeV $^{-2}$ in agreement with expectations from Regge phenomenology. The quality of the fit is similar to the one we achieved for the Dirac form factors. We find a very large range of allowed fit parameters, which is hardly surprising since we have to determine both functions $e_v^q(x)$ and $g_q(x)$ in (19). An important reduction of the allowed parameter space is due to the positivity bound (18) and its analog in impact parameter space at large x (where it is reasonable to neglect the contribution from antiquarks, which is subtracted in the valence distributions and invalidates positivity conditions if it is large). We find in particular that $\beta_u \geq 3.5$ and $\beta_d \geq 5$ is required with our ansatz, which quantifies our above statement that E_v^q must rather strongly decrease with x .

We can now evaluate the orbital angular momentum carried by valence quarks in the proton, which according to Ji's sum rule [17] is

$$L_v^q = \frac{1}{2} \int_0^1 dx \left[x e_v^q(x) + x q_v(x) - \Delta q_v(x) \right]. \quad (21)$$

With our simple ansatz (20) one readily obtains

$$\int_0^1 dx x e_v^q(x) = \kappa_q (1 - \alpha) / (2 - \alpha + \beta_q). \quad (22)$$

Remarkably, the results for L_v^u and L_v^d show only little variation in the range of parameters α , β_u and β_d for which we achieve a good fit to the Pauli form factors, as shown in Fig. 10. For the isovector combination we obtain a rather well determined value $L_v^u - L_v^d = -\frac{1}{2}$ (0.77 to 0.92). The isoscalar combination $L_v^u + L_v^d = -\frac{1}{2}$ (0.11 to 0.22) has a large uncertainty and is rather small, due to partial cancellation between the two quark flavors. Lattice calculations by the QCDSF Collaboration obtain $L^u - L^d = -\frac{1}{2} (0.90 \pm 0.12)$ and $L^u + L^d$ compatible with zero within errors [15]. We find the agreement with our estimates encouraging, especially for the isovector combination, where contributions from sea quarks should be small.

As in the case of H_v^q , we find that the different behavior of E_v^u and E_v^d at large x is reflected in a different t dependence of their moments, as is characteristic for the Feynman mechanism. This is seen in the lower panels of Fig. 8, where we plot

$$e_i^q(t) = \int_0^1 dx x^{i-1} E_v^q(x, t) \quad (23)$$

for $i = 1, 2, 3$ obtained with our best fit, where the large- x powers in (20) are $\beta_u \approx 4$ and $\beta_d \approx 5.6$. It will be very interesting to see whether such a behavior can be established in form factor measurements or lattice calculations.

Let us finally comment on the behavior of the ratio F_2^p/F_1^p for $|t|$ up to about 6 GeV 2 , where there is data from the polarization transfer

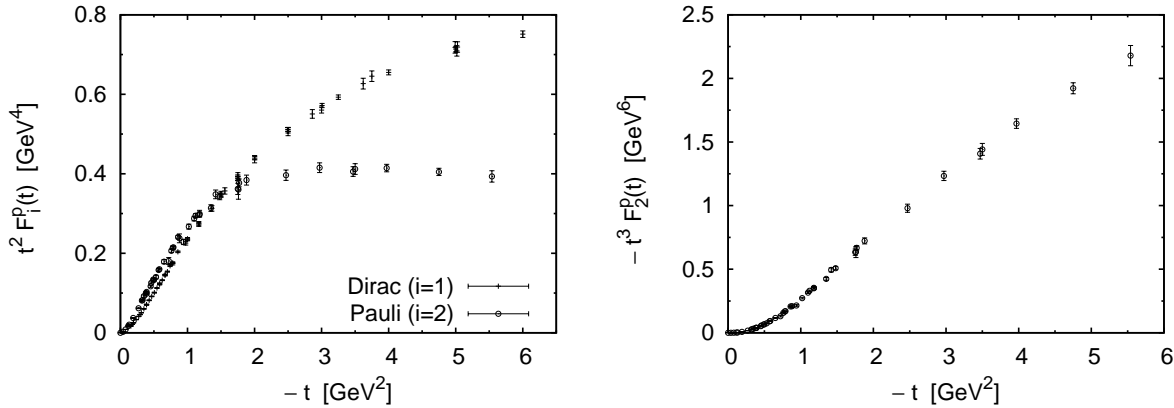


Figure 11. Data for the proton form factors, scaled by t^2 (left) or $|t|^3$ (right). The plateau of $t^2 F_2^p(t)$ for $|t|$ between 2 and 6 GeV^2 illustrates that, in a limited kinematic region, observables may exhibit an approximate power law which is only transient and very different from their asymptotic behavior.

method [18]. This data is rather well described by a behavior $F_2^p/F_1^p \sim |t|^{-1} \log^2(|t|/\Lambda^2)$ with $\Lambda \approx 300$ MeV, suggested by the recent study [19] of F_2^p in the leading-twist hard-scattering mechanism [20]. For the individual form factors, this study obtains an approximate behavior

$$\begin{aligned} F_1(t) &\sim \alpha_s^{2+32/(9\beta)} |t|^{-2}, \\ F_2(t) &\sim \alpha_s^{2+8/(3\beta)} \log^2(|t|/\Lambda^2) |t|^{-3}, \end{aligned} \quad (24)$$

where the squared logarithm in F_2 arises from cutting off endpoint singularities in the integrations over quark momentum fractions. The terms with $\beta = 11 - 2n_f/3$ in the exponents are due to the evolution of the proton distribution amplitude and numerically small, with $32/(9\beta) \approx 0.4$ and $8/(3\beta) \approx 0.3$. If one takes α_s at scale t , then the logarithms in F_2 approximately cancel and $|t|^3 F_2(t)$ should be nearly t independent. If in contrast one assumes that the relevant scale in α_s is so low that the running coupling is effectively frozen, then $|t|^2 F_1(t)$ should be flat. Figure 11 shows that neither behavior is realized for $|t|$ below 6 GeV^2 , where both $|t|^3 F_2^p(t)$ and $|t|^2 F_1^p(t)$ increase. Thus, a calculation of F_1^p and F_2^p at leading twist and leading order in α_s not only underestimates the normalization of the form factors (as remarked in [19]) but also fails to describe their t dependence in the region under discussion. Whether the fact that the ratio F_2^p/F_1^p can be

described with (24) is fortuitous or a sign of precious scaling behavior remains a matter of debate. An important source of power corrections is the effect of transverse quark momentum in the hard-scattering subprocess [21]. This effect decreases the form factors more strongly at lower than at higher $|t|$, which may improve the description of the t dependence but makes the discrepancy for their normalization worse. The contribution of the Feynman mechanism to F_1^p and F_2^p originates from different kinematic configurations than the hard-scattering mechanism. As a correction to the leading-twist result it is hence additive rather than multiplicative and will therefore not obviously cancel in the form factor ratio.

Acknowledgments

It is a pleasure to thank D. Leinweber, L. von Smekal and T. Williams for organizing an excellent workshop. I am grateful to D. Brömmel for a careful reading of the manuscript. This work is supported by the Helmholtz Association, contract number VH-NG-004.

REFERENCES

1. M. Diehl, Phys. Rept. **388**, 41 (2003) [hep-ph/0307382]; A. V. Belitsky and A. V. Radyushkin, hep-ph/0504030.

2. D. E. Soper, Phys. Rev. D **5**, 1956 (1972);
Phys. Rev. D **15**, 1141 (1977).
3. M. Burkardt, Phys. Rev. D **62**, 071503 (2000), Erratum ibid. D **66**, 119903 (2002) [hep-ph/0005108].
4. M. Diehl, Eur. Phys. J. C **25**, 223 (2002), Erratum ibid. C **31**, 277 (2003) [hep-ph/0205208].
5. A. V. Belitsky, X. D. Ji and F. Yuan, Phys. Rev. D **69**, 074014 (2004) [hep-ph/0307383].
6. M. Diehl, T. Feldmann, R. Jakob and P. Kroll, Eur. Phys. J. C **39**, 1 (2005) [hep-ph/0408173].
7. M. Burkardt, Phys. Lett. B **595**, 245 (2004) [hep-ph/0401159].
8. M. Guidal, M. V. Polyakov, A. V. Radyushkin and M. Vanderhaeghen, Phys. Rev. D **72**, 054013 (2005).
9. J. Pumplin *et al.*, JHEP **0207**, 012 (2002) [hep-ph/0201195].
10. K. Goeke, M. V. Polyakov and M. Vanderhaeghen, Prog. Part. Nucl. Phys. **47**, 401 (2001) [hep-ph/0106012].
11. S. Chekanov *et al.* (ZEUS Collab.), *Nucl. Phys.* **B 695**, 3 (2004) [hep-ex/0404008];
A. Aktas *et al.* (H1 Collab.), hep-ex/0510016.
12. R. P. Feynman, *Photon-Hadron Interactions*, Benjamin, New York, 1972.
13. M. Gökeler *et al.* (QCDSF Collab.), Phys. Rev. Lett. **92**, 042002 (2004) [hep-ph/0304249].
14. P. Hägler *et al.* (LHPC Collab.), Phys. Rev. D **68**, 034505 (2003) [hep-lat/0304018];
Phys. Rev. Lett. **93**, 112001 (2004) [hep-lat/0312014].
15. G. Schierholz, these proceedings.
16. M. Burkardt, Phys. Lett. B **582**, 151 (2004) [hep-ph/0309116].
17. X. D. Ji, Phys. Rev. Lett. **78**, 610 (1997) [hep-ph/9603249].
18. O. Gayou *et al.* (Jlab Hall A Collab.), Phys. Rev. Lett. **88**, 092301 (2002) [nucl-ex/0111010].
19. A. V. Belitsky, X. D. Ji and F. Yuan, Phys. Rev. Lett. **91**, 092003 (2003) [hep-ph/0212351].
20. G. P. Lepage and S. J. Brodsky, Phys. Rev. D **22** (1980) 2157.
21. J. Bolz, R. Jakob, P. Kroll, M. Bergmann and N. G. Stefanis, Z. Phys. C **66**, 267 (1995) [hep-ph/9405340].